ACS APPLIED MATERIALS & INTERFACES

Research Article

Cite This: ACS Appl. Mater. Interfaces XXXX, XXX, XXX−XXX

www.acsami.org

Conductive Shape Memory Microfiber Membranes with Core−Shell Structures and Electroactive Performance

Fenghua Zhang,[†,§] Yuliang Xia,[†,§] Linlin Wang,[†] Liwu Liu,[‡] Yanju Liu,[‡] and Jinsong Leng*[,†]

[†]Centre for Composite Materials and Structures, Harbin Institute of Technology (HIT), P.O. Box 3011, No. 2 Yikuang Street, Harbin 150080, People's Republic of China

[‡]Department of Astronautic Science and Mechanics, Harbin Institute of Technology (HIT), P.O. Box 301, No. 92 West Dazhi Street, Harbin 150001, People's Republic of China

Supporting Information

ABSTRACT: Conductive shape memory polymers as a class of functional materials play a significant role in sensors and actuators. A high conductivity and a high response speed are needed in practical applications. In this work, a conductive shape memory polylactic acid (PLA) microfiber membrane was synthesized by combining electrospinning with chemical vapor polymerization. The shape memory PLA was electrospun into microfibers with different diameters, and a conductive polypyrrole (PPy) coating was applied to the PLA microfiber membranes using vapor polymerization. The conductivity of the microfiber membrane was investigated as a function of different experimental parameters: $FeCl_3$ concentration, PPy evaporation time, and PPy temperature. The maximum conductivity of the membrane prepared in a sub-zero environment is 0.5 S/cm, which can sustain a heat-generating electric current sufficient to trigger the electro-actuated behaviors of the membrane within 2 s at 30 V. Thermographic imaging was used to assess the uniformity of the temperature distribution during the shape recovery process. The low surface temperature is compatible with potential applications in many fields.

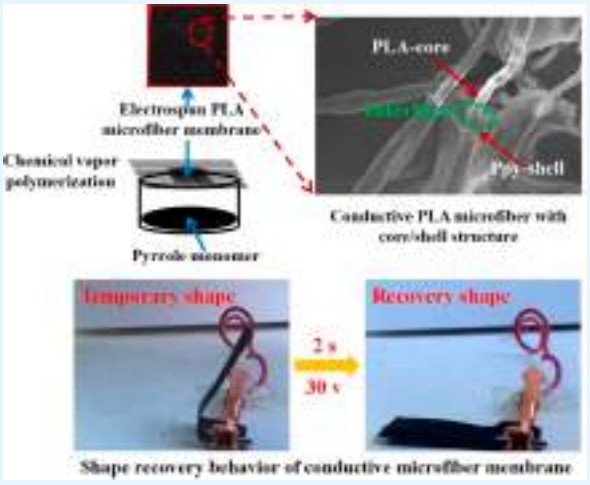

KEYWORDS: *shape memory polymers, conductive microfiber membranes, composites, electrical actuation, electrospinning*

INTRODUCTION

As a class of smart active materials, shape memory polymers (SMP) can be deformed into any shape when heated to a set transition temperature yet can revert to the original shape when exposed to a variety of external stimuli, including heat, humidity, light, pressure, solvents, microwaves, and electrical and magnetic fields.[1−5] SMPs and their composites have attracted an increasing amount of attention because of their deformation and shape changing properties in addition to their light weight, easy processing, and low cost. Combining smart polymers and morphing structures, SMPs have potential applications in a wide range of fields, including aerospace, robotics, and biomedical science. In aerospace engineering, SMPs can be used to create active hinges that support antennae, reflectors, and solar arrays.[6] In the biomedical world, SMP nanoparticles, fibrous scaffolds, and four-dimensional printed complex structures are being developed for controlled drug release and tissue engineering applications.[7−11] For identification and authentication applications, SMPs have been used as switchable information carriers (e.g., two-dimensional barcodes) that permit display and decoding of information only upon exposure to environmental stimuli.[12] The applications of SMPs and their composites are continuously expanding to encompass more and more fields.[13−16]

To meet the real needs of practical applications, remote-controlled actuation of SMPs is necessary, especially electrical actuation. To this end, conductive particles, including carbon nanotubes,[17] carbon black,[18] and carbon nanofibers[19] as well as graphene,[20] have been mixed with shape memory polymers to create conductive hybrid materials that can reach the transition temperature through internal heating following application of an electrical potential difference. In addition, nickel has been added to shape memory polymers to create a hybrid material that can be triggered in the presence of a magnetic field.[21,22] Other techniques have included selective heating of active shape recovery elements through selective surface light absorption. Application of black ink to the polymer surface provides an area of preferential absorption that increases the local temperature upon exposure to infrared light.[23] A general limitation of these additive-based approaches has arisen because of the non-uniform distribution of fillers. Therefore, there is a significant impetus to develop new structures suited to electrical actuation. Structures based on composite fibers with a core−shell

Received: July 28, 2018
Accepted: September 24, 2018
Published: September 24, 2018

DOI: 10.1021/acsami.8b12743
ACS Appl. Mater. Interfaces XXXX, XXX, XXX−XXX

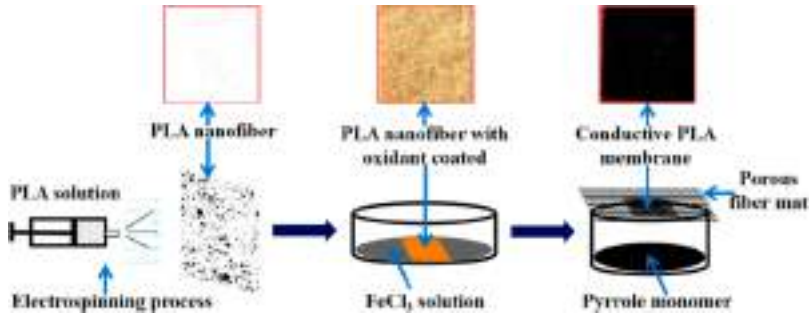

Figure 1. Workflow for the preparation of conductive membranes.

composition offer a promising avenue; they have the potential to achieve a relatively uniform temperature when electrically activated, and the conductivity can be adjusted by changing the material properties and morphology of the constituent core–shell components.

To date, SMPs have been developed using various materials, including thermosetting and thermoplastic polymers. Polylactic acid (PLA) is one such polymer and is particularly suited to biomedical applications because of its biocompatible and biodegradable nature. For applications that require electroactuation, conductive polymers form ideal fabrication materials.[24,25] Fabrication of conductive fibers has been performed with a range of different conductive polymers.[26] Among the various conductive polymers, polypyrrole (PPy) has the highest conductivity and is also perfectly stable. Pyrrole has been widely investigated in energy storage applications.[27−29] It is hard to dissolve PPy in any solvent, and the traditional method of fabricating PPy is to mix ferrite with pyrrole.[30,31] Combining PPy with a shape memory polymer is an ideal way to fabricate a conductive shape memory material.

In this work, we fabricated conductive shape memory microfiber membranes using conductive fibers with a composite core–shell structure. The shape memory microfiber "core" was prepared by electrospinning PLA with different concentrations. Chemical vapor polymerization was then used to deposit a conductive PPy "shell" on the electrospun microfibers and produce conductive shape memory microfibers that could be formed into conductive membranes. The electroactive behavior of the conductive microfiber membranes was then investigated. The morphology, structure, and thermodynamics were all analyzed, and the temperature distribution of the conductive microfiber membrane during the shape recovery process was assessed. Because of the favorable biological properties of the materials, the resulting shape memory membranes have potential applications in the biomedical field, including tissue engineering and regenerative medicine for the treatment of heart disease.

EXPERIMENTAL SECTION

Materials. Polylactic acid (PLA) (BIO PLUS 6201D) was purchased from Nature Works Corp. Isopropanol (AR) and chloroform were purchased from Fuyu Fine Chemical Co. Pyrrole (reagent grade, 98%) was purchased from Sigma-Aldrich Corp. Iron chloride ($FeCl_3$) (anhydrous, 98%) was purchased from Alfa Aesar. All the chemicals were used directly without further treatment.

Electrospinning of PLA Microfibers. PLA microfibers were fabricated by electrospinning (FM-12, FuYouMa Co.) under the following conditions. The PLA was dissolved in chloroform at concentrations from 10 to 14%. The applied voltages and collecting distance for electrospinning were 15–25 kV and 15 cm, respectively. The liquid flow speed was 1.5–2.5 mL/h. The resulting microfiber membranes were collected for 2 h and then placed in an oven at 40 °C to evaporate the solvent.

Fabrication of Conductive Shape Memory Microfiber Membranes. The experimental setup and workflow used for fabricating the conductive SMP microfiber membranes are illustrated in Figure 1. There are three steps: (1) electrospinning of the microfiber membranes, (2) immersion of the membranes in an $FeCl_3$ solution, and (3) evaporating the pyrrole monomer onto the membranes following treatment with $FeCl_3$. Solutions of $FeCl_3$ in isopropanol with concentrations of 5, 10, and 15% were prepared. The electrospun PLA microfiber membrane was cut into 5 cm × 5 cm pieces and then immersed in the $FeCl_3$ solution for 2–16 min. The membrane was then dried at room temperature for 30 min and then transferred onto a breathable porous mat atop a beaker containing 0.5–2 mL of pyrrole. Polymerization was then performed under different temperature and time conditions to obtain the conductive microfiber membranes. Finally, the conductive SMP microfiber membranes were dipped into deionized (DI) water to remove the $FeCl_3$ to improve the conductivity. The thickness of the membranes varied from 30 to 100 μm.

Characterization. The morphology and microstructure of the conductive SMP microfiber membranes were captured using a scanning electron microscope (TESCAN, VEGA3 SB) at 20 kV. A PerkinElmer Spectrum Two Fourier transform infrared (FT-IR) spectrometer was then used to investigate the samples by generating FT-IR spectra using the attenuated total reflectance method. The spectra were obtained under room conditions at a resolution of 2 cm^{-1} with 40 scans for each characterization. Differential scanning calorimeter measurements (DSC 1 STAR System, Mettler-Toledo) were performed under nitrogen. The samples were first heated from 0 to 250 °C and then cooled to 0 °C at a rate of 10 °C/min. Thermogravimetric analysis (TGA) (TGA/DSC 1 STAR System, Mettler-Toledo) was performed with samples heated from 25 to 500 °C at a rate of 10 °C/min in a nitrogen atmosphere. The conductivity of the SMP microfiber membranes was assessed using a four-point probe (Napson Corp., RT-70 V/RG-7C). An average value derived from 20 independent measurements was used. Infrared thermographic images were captured using an infrared camera (JENOPTIK InfraTec) to assess the temperature distribution of samples with different conductivities, including the temperature distribution during the shape recovery process. The mechanical properties of the films were tested using a dynamic mechanical analyzer in force control mode (DMA Q800 apparatus, TA Instruments) at 25 °C and a force rate of 1.0 N/min.

The shape memory and recovery performance of the SMP microfiber membranes were analyzed by applying a voltage at opposing sides of the conductive film (ITECH DC, Source Meter). The membrane was first cut into a "U" shape such that the current flow would pass through the mechanical buckling point. After application of 25 V, the stimulus was sufficient to heat the membrane to the glass transition temperature and the membrane was folded, while an additional electrical stimulus from 25 to 40 V was sufficient to trigger shape recovery of the hybrid membrane.

RESULTS AND DISCUSSION

Morphology and Microstructures. The microfiber membrane fabrication process outlined above produced a core–shell

DOI: 10.1021/acsami.8b12743
ACS Appl. Mater. Interfaces XXXX, XXX, XXX−XXX

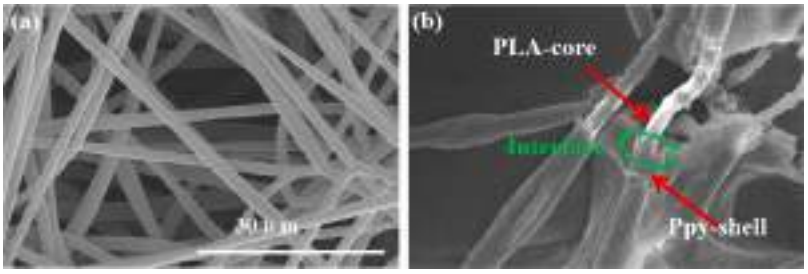

Figure 2. SEM images of (a) PLA microfibers and (b) conductive microfibers coated with PPy.

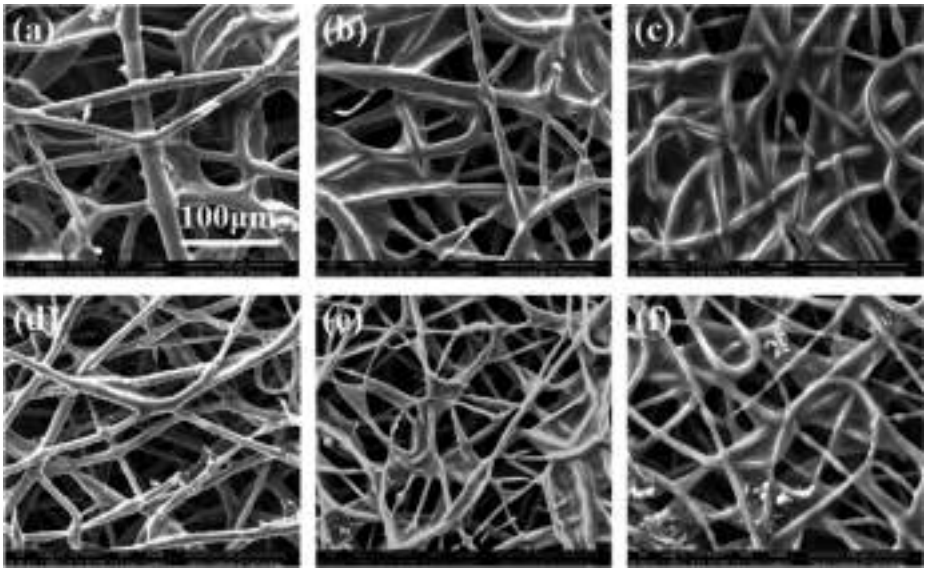

Figure 3. SEM images of conductive microfibers under different conditions following immersion in a 10% $FeCl_3$ solution for 5 min: (a) evaporating PPy at 20 °C for 2 h, (b) evaporating PPy at 40 °C for 2 h, (c) evaporating PPy at 60 °C for 2 h, (d) evaporating PPy at 0 °C for 1 h, (e) evaporating PPy at 0 °C for 3 h, and (f) evaporating PPy at 0 °C for 4 h.

structure for the constituent fibers in which a PLA "core" was coated with a PPy "shell". This structure is apparent in the scanning electron microscopy (SEM) images shown below. Figure 2a shows a SEM image of the electrospun PLA microfibers; the uniform diameter distribution and smooth surface finish of the fibers are apparent. The diameter is around 1.5 μm. The conductive PLA microfibers were obtained by immersing the electropun microfibers in a 10% $FeCl_3$ solution for 5 min and coating with a PPy monomer at 0 °C for 2 h. Figure 2b clearly illustrates the core−shell structure of these coated fibers and is in keeping with the multistep fabrication process. The core is a pure nonconductive PLA fiber, and the shell is a PPy coating layer that acts as the conductive element in this composite material.

SEM images were captured to understand the effect of the coating conditions on the microstructure of the composite microfibers. Figure 3 shows images of the PPy-coated PLA membranes under various conditions. The PPy coating is a result of a chemical vapor reaction, and panels a−c of Figure 3 show the result of this reaction at different temperatures. The degree of coating increases as the temperature increases, and at 60 °C, the coating extends to form a film between fibers rather than just individual microfibers (Figure 3c). The effect of coating time on the morphology of the microfibers was also investigated, and panels d−f of Figure 3 show the effect of changing the coating time from 1 to 4 h. It is apparent that the temperature and time have a significant impact on the morphology and structure of the microfibers, which in turn will have an impact on the conductivity of the membranes. In addition, the distribution of diameters, the average diameter, and the standard deviation for pure PLA fibers and conductive fibers were measured. The results demonstrate that the average diameter increases as the coating time increases as shown in Figure S1.

Chemical and Thermal Properties. FT-IR spectra were obtained as shown in Figure 4a to characterize the molecular structure of the PLA and PPy. The peaks at 3500−3000 cm^{-1} were ascribed to O−H stretching. The peak around 2900 cm^{-1} was assigned to a C−H stretching vibration. The peaks at 1451 and 920 cm^{-1} were attributed to C═O and C−O−C functional groups, respectively, that can be clearly observed in PLA spectrum analysis. The peaks at 1482 and 1788 cm^{-1} were attributed to N−H stretching vibrations. The peaks at 1680 and 1397 cm^{-1} corresponded to C═C and C−C PPy ring variations, respectively. The peak at 1280 cm^{-1} was attributed to C−N vibrations. Similar IR peaks have been reported in another paper.[32] The thickness of the PPy coating increases as the pyrrole exposure time is extended. Hence, the transmittance of the sample decreases as the coating time increases.

Differential scanning calorimetry (DSC) experiments were performed with pure PLA and PPy-coated membranes to explore the thermal transitions in these materials. As shown in Figure 4b, the transition temperature of pure PLA is around 70 °C. In comparison, the transition temperature of the coated microfiber membranes is slightly decreased. The membrane

DOI: 10.1021/acsami.8b12743
ACS Appl. Mater. Interfaces XXXX, XXX, XXX−XXX

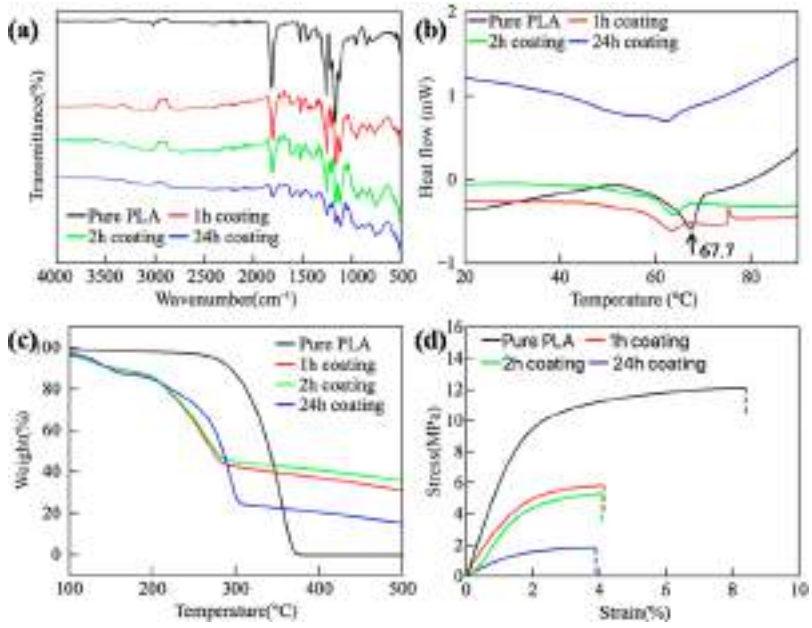

Figure 4. (a) FT-IR spectra, (b) differential scanning calorimetry images, (c) TGA images, and (d) mechanical properties of pure PLA membranes and PPy-coated membranes. The coating temperature was −20 °C.

crystallization temperature was not visible in the traces because of the the small sample quantity. The thermal stability of the core−shell PLA/PPy composite microfibers was determined by TGA, as shown in Figure 4c. The degradation temperature of pure PLA is around 300 °C, which can be contrasted with a PPy coating degradation temperature of around 200 °C. Weight loss was apparent for the PPy-coated membrane at temperatures below the degradation temperature. In addition, the mechanical properties of conductive membranes with different polymerization times were characterized. In comparison to that of pure PLA fibrous membranes, it is apparent from the tension testing result shown in Figure 4d that the mechanical properties of conductive coated membranes degrade as the PPy coating time increases. After coating with PPy had been performed for 24 h, the mechanical degradation was such that the membranes became brittle.

Conductivity of PLA Microfiber Membranes. Microfiber membrane samples were fabricated under a range of conditions to explore the parameter space and understand the factors that impacted membrane conductivity (Figure 5a−d). In all cases, except the variable parameter, the fixed conditions were as follows. The PLA concentration for electrospinning was 12%. The concentration of the $FeCl_3$ solution was 15%. The PLA was rinsed in an $FeCl_3$ solution for 5 min. The polymerization time was 2 h. The polymerization temperature was −20 °C. Electrospinning is the first step in the preparation of the conductive fibers. The concentration of the PLA solution used during this step can affect two factors that determine the conductivity of the membrane: the consistency and the diameter of the microfibers. As the concentration of the PLA solution decreases, it becomes easier to form microfibers, leading to an increase in the consistency of the fibers as well as a decrease in the diameter.[5] This results in more electric circuits as the PPy shell structure forms on the PLA scaffolds. Thinner PLA fibers lead to a denser network of fibers, which in turn lead to more electrical conduction paths, resulting in an overall increase in the conductivity of the membrane with a decreasing concentration of the PLA solution, as shown in Figure 5a.

Besides the concentration of the PLA solution, there are other factors that also affect the conductivity of the hybrid membrane. Following electrospinning, the resulting PLA membrane is immersed in an $FeCl_3$ solution. The $FeCl_3$ is adsorbed onto the surface of the microfibers where it catalyzes the pyrrole polymerization reaction that is used to create the core−shell conductive structure. The adsorbed $FeCl_3$ promotes formation of conductive PPy, and the conductivity of the resulting hybrid membrane depends strongly on the concentration of the $FeCl_3$ solution and on the length of time that the PLA membrane is dipped into the $FeCl_3$ solution (see panels a and b of Figure 5). As the concentration of $FeCl_3$ increases, more $FeCl_3$ is adsorbed onto the PLA fiber surface, which accelerates the formation of pyrrole and increases the conductivity of the membranes (Figure 5a). The adsorption time also strongly affects the membrane conductivity. The conductivity increases as the adsorption time increases until 8 min, when the adsorption equilibrium is reached and the conductivity plateaus (Figure 5b).

A further factor that affects the conductivity is the temperature of the polymerization reaction. An increase in the temperature will accelerate the polymerization reaction but also results in more side reactions. Hence, for this reaction, a sub-zero environment is necessary to create a uniform conductive shell with a smooth surface finish that can enclose the PLA fiber (see Figure 5c). Higher-temperature environments will lead to a nonuniform surface on the microfibers as can be seen in the SEM images in Figure 2. An additional factor that affects conductivity is the polymerization time as shown in Figure 5d. It can be seen that the conductivity increases as the polymerization time increases but reaches a limit after reaction for 12 h in a sub-zero environment.

The $FeCl_3$ acts as a catalyst when pyrrole is polymerized on the surface of the PLA. Hence, if the $FeCl_3$ is not removed following the polymerization reaction, it can tend to remain in place at the PLA/PPy core−shell boundary and gradually absorb water from the air as time passes. This can easily lead to formation of crystalline hydrates that stick to the container holding the membrane. Following polymerization, the membrane is

DOI: 10.1021/acsami.8b12743
ACS Appl. Mater. Interfaces XXXX, XXX, XXX−XXX

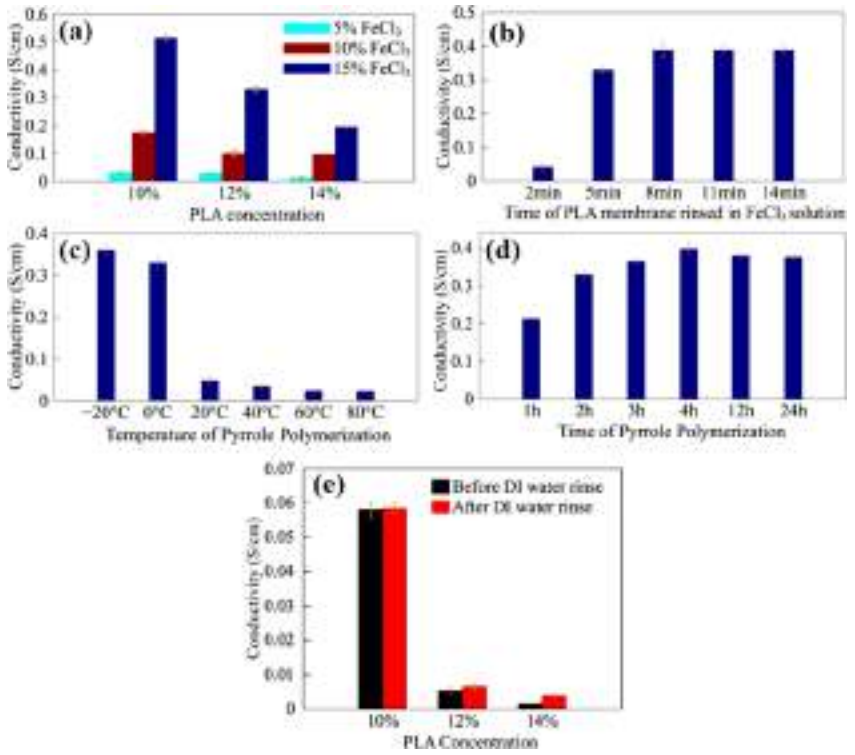

Figure 5. Factors that affect the electrical conductivity of microfiber membranes: (a) effect of the PLA solution concentration and $FeCl_3$ concentration, (b) effect of varying the PLA rinsing time in the $FeCl_3$ solution, (c) effect of varying the pyrrole polymerization temperature, (d) effect of varying the pyrrole polymerization time, and (e) effect of $FeCl_3$ extraction.

therefore rinsed in DI water for 60 s to extract the $FeCl_3$, a process that leads to a visible yellow coloration in the DI water. Figure 5e demonstrates that postpolymerization rinsing can increase the conductivity of the conductive membrane and that the higher the prerinse resistivity, the greater the relative magnitude of the change in pre/postrinse conductivity. There are two reasons for this. First, $FeCl_3$ is nonconductive, and removal of $FeCl_3$ will therefore decrease the contact resistivity. Second, the microfibers expand during the rinsing process, leading to a 20−30% increase in the thickness of the membrane, so $FeCl_3$ removal results in the formation of more circuit contact points. As the concentration of PLA decreases, the fiber diameter decreases and the fiber network becomes more dense, which results in it having enough circuit points to support electrical current transfer even without postrinsing. However, at increased PLA concentrations, the fiber network is less dense and the number of circuit points decreases correspondingly. The new circuit points generated as a result of the postrinsing therefore help to increase the conductivity of the fiber network. The sample used for the tests in Figure 5e was fabricated under the same conditions listed above, except that the polymerization temperature was 20 °C rather than −20 °C.

Electroactive Shape Memory Behaviors. The conductive membrane was cut into an initial "U" shape with a 0.5 cm × 1 cm rectangular gap between the arms of the "U". The thickness and conductivity of the membrane were 40 μm and 0.5 S/cm, respectively. Application of a 25 V potential difference across the arms of the "U" allowed the membrane to reach the transition temperature after 3 s, at which stage the membrane was folded, and the deformation was maintained for 1 min while cooling o room temperature with the electrical stimulation removed, resulting in the temporary shape shown in Figure 6i. The shape recovery process was captured on video (see the Supporting Information), and Figure 6 shows the shape recovery behavior of the conductive microfiber membrane over the course of 2 s. The recovery is very rapid. The shape recovery time was measured as a function of applied voltage at 15, 20, 25, 30, 35, and 40 V. Above 40 V, the heating effect increases to a level that can damage the membrane. Hence, the maximum voltage was limited to 40 V. Furthermore, practical applications for microfiber membranes point to safe working voltages of <36 V.

Figure 7a shows the shape recovery time as a function of applied voltage for the sample with a conductivity of 0.35 S/cm. As the voltage increases, the shape recovery time decreases because the membrane reaches its transition temperature more quickly. The minimum voltage required for partial shape recovery is 15 V, albeit with an extended shape recovery time of 90 s, whereas at 40 V, the microfiber membrane can fully recover its original shape in 2 s. Thermal infrared images were captured for different applied voltages, as shown in Figure 7b. The color map charts the distribution of temperatures, and one can see that the temperature distribution is relatively uniform. One can also see that the temperature of the membrane increases rapidly from room temperature to the transition temperature. This is because the membrane is very thin and can therefore be heated or cooled in a short period of time.

In addition to the characterization of the shape memory behavior of the PLA/PPy composite material, the shape memory performance of pure PLA was also investigated for comparative purposes, both on a heating stage and in hot water at 70 °C. Rapid shape recovery times of <5 s were observed, as shown in Figure S2. The shape memory recovery performance for pure PLA is therefore similar to that of the PLA/PPy composite membrane material when activated with applied voltages of 35−40 V.

DOI: 10.1021/acsami.8b12743
ACS Appl. Mater. Interfaces XXXX, XXX, XXX−XXX

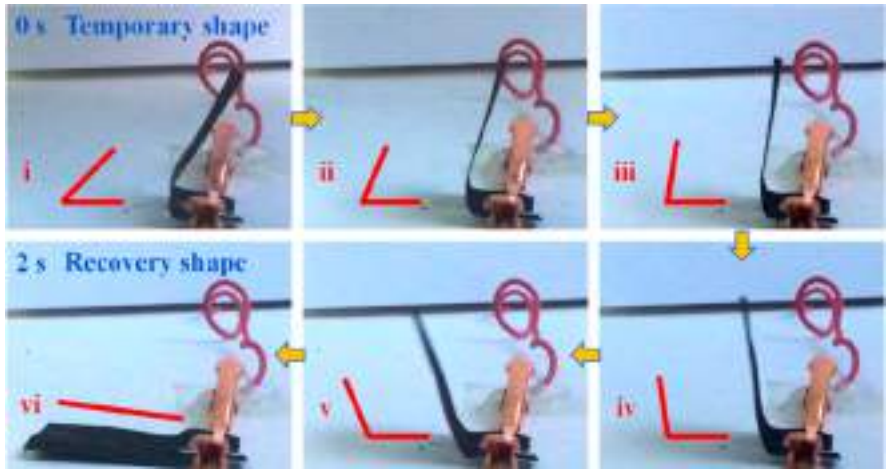

Figure 6. Shape recovery process of the conductive microfiber membrane at 30 V.

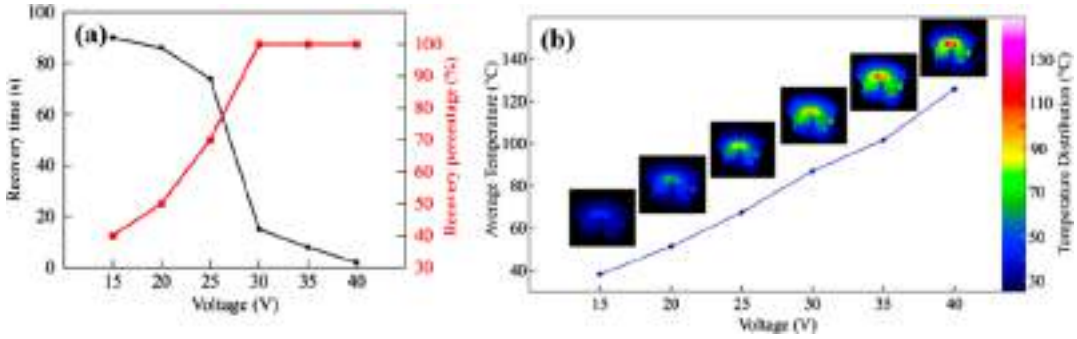

Figure 7. (a) Relationship between applied voltages and shape recovery time and (b) relationship between the applied voltage and surface temperature.

This work has focused on the electrically induced shape memory behavior of conductive structures formed from composite fibers with a core−shell composition: an inner fiber "core" formed from a shape memory polymer (PLA) and an outer "shell" formed from a conductive polymer (PPy). Pure PLA is nonconductive and therefore not amenable to electro-acutation when used alone, while pure PPy does not possess any inherent shape memory properties. A PLA/PPy composite material that combines the properties of both base materials is therefore an effective way to form a conductive shape memory material. The shape memory properties of the composite material are similar to those of pure PLA, with the added benefit that shape recovery can be triggered through electro-actuation.

CONCLUSIONS

We investigated the preparation and behavior of conductive shape memory microfiber membranes formed using composite core−shell structure microfibers of PLA coated with PPy. The morphology and conductivity of the microfiber membranes were impacted by various fabrication parameters, a number of which were explored as part of this study, including effects of the $FeCl_3$ concentration, the PPy evaporation time, and the PPy temperature. The maximum conductivity of the membranes was 0.5 S/cm, sufficient to allow electro-activated heating of the membrane and triggering of the shape memory recovery process through application of a relatively low applied voltage. A stimulus of 30 V was able to achieve full shape recovery in 2 s with a relatively uniform heating distribution across the membrane surface. The shape memory properties and electro-active behavior of these conductive membranes make them suitable for use in shape stimulus responsive applications, biomedical areas, and other areas.

ASSOCIATED CONTENT

Supporting Information

The Supporting Information is available free of charge on the ACS Publications website at DOI: 10.1021/acsami.8b12743.

Figures S1 and S2 (PDF)

Movie of the shape recovery process (AVI)

AUTHOR INFORMATION

Corresponding Author

*E-mail: lengjs@hit.edu.cn. Fax: +86 451 8640 2328.

ORCID

Jinsong Leng: 0000-0001-5098-9871

Author Contributions

§F.Z. and Y.X. contributed equally to this work.

Notes

The authors declare no competing financial interest.

ACKNOWLEDGMENTS

This work is supported by the National Natural Science Foundation of China (Grants 11632005, 11672086, 11802075, and 11772109).

DOI: 10.1021/acsami.8b12743
ACS Appl. Mater. Interfaces XXXX, XXX, XXX−XXX

REFERENCES

(1) Xiao, X.; Kong, D.; Qiu, X.; Zhang, W.; Liu, Y.; Zhang, S.; Zhang, F.; Hu, Y.; Leng, J. Shape Memory Polymers with High and Low Temperature Resistant Properties. *Sci. Rep.* **2015**, *5*, 14137.

(2) Zhang, F.; Zhang, Z.; Liu, Y.; Cheng, W.; Huang, Y.; Leng, J. Thermosetting Epoxy Reinforced Shape Memory Composite Microfiber Membranes: Fabrication, Structure and Properties. *Composites, Part A* **2015**, *76*, 54−61.

(3) Wei, H.; Zhang, Q.; Yao, Y.; Liu, L.; Liu, Y.; Leng, J. Direct-Write Fabrication of 4d Active Shape-Changing Structures Based on a Shape Memory Polymer and Its Nanocomposite. *ACS Appl. Mater. Interfaces* **2017**, *9* (1), 876−883.

(4) Wang, L.; Yang, X.; Chen, H.; Gong, T.; Li, W.; Yang, G.; Zhou, S. Design of Triple-Shape Memory Polyurethane with Photo-Cross-Linking of Cinnamon Groups. *ACS Appl. Mater. Interfaces* **2013**, *5* (21), 10520−10528.

(5) Zhang, F.; Zhang, Z.; Liu, Y.; Leng, J. Shape Memory Properties of Electrospun Nafion Nanofibers. *Fibers Polym.* **2014**, *15* (3), 534−539.

(6) Santo, L.; Quadrini, F.; Ganga, P. L.; Zolesi, V. Mission Bion-M1: Results of Ribes/Foam2 Experiment on Shape Memory Polymer Foams and Composites. *Aerosp. Sci. Technol.* **2015**, *40*, 109−114.

(7) Balk, M.; Behl, M.; Wischke, C.; Zotzmann, J.; Lendlein, A. Recent Advances in Degradable Lactide-Based Shape-Memory Polymers. *Adv. Drug Delivery Rev.* **2016**, *107*, 136−152.

(8) Kai, D.; Prabhakaran, M. P.; Yu Chan, B. Q.; Liow, S. S.; Ramakrishna, S.; Xu, F.; Loh, X. J. Elastic Poly(Epsilon-Caprolactone)-Polydimethylsiloxane Copolymer Fibers with Shape Memory Effect for Bone Tissue Engineering. *Biomed. Mater. (Bristol, U. K.)* **2016**, *11* (1), 015007.

(9) Bao, M.; Lou, X.; Zhou, Q.; Dong, W.; Yuan, H.; Zhang, Y. Electrospun Biomimetic Fibrous Scaffold from Shape Memory Polymer of Pdlla-Co-Tmc for Bone Tissue Engineering. *ACS Appl. Mater. Interfaces* **2014**, *6* (4), 2611−21.

(10) Tseng, L. F.; Mather, P. T.; Henderson, J. H. Shape-Memory-Actuated Change in Scaffold Fiber Alignment Directs Stem Cell Morphology. *Acta Biomater.* **2013**, *9* (11), 8790−801.

(11) Shah, N. J.; Geiger, B. C.; Quadir, M. A.; Hyder, N.; Krishnan, Y.; Grodzinsky, A. J.; Hammond, P. T. Synthetic Nanoscale Electrostatic Particles as Growth Factor Carriers for Cartilage Repair. *Bioeng. Transl. Med.* **2016**, *1* (3), 347−356.

(12) DiOrio, A. M.; Luo, X.; Lee, K. M.; Mather, P. T. A Functionally Graded Shape Memory Polymer. *Soft Matter* **2011**, *7* (1), 68−74.

(13) Meng, Q.; Hu, J. A Review of Shape Memory Polymer Composites and Blends. *Composites, Part A* **2009**, *40* (11), 1661−1672.

(14) Liu, Y.; Lv, H.; Lan, X.; Leng, J.; Du, S. Review of Electro-Active Shape-Memory Polymer Composite. *Compos. Sci. Technol.* **2009**, *69* (13), 2064−2068.

(15) Meng, H.; Li, G. A Review of Stimuli-Responsive Shape Memory Polymer Composites. *Polymer* **2013**, *54* (9), 2199−2221.

(16) Liu, Y.; Du, H.; Liu, L.; Leng, J. Shape Memory Polymers and Their Composites in Aerospace Applications: A Review. *Smart Mater. Struct.* **2014**, *23* (2), 023001.

(17) Cho, J. W.; Kim, J. W.; Jung, Y. C.; Goo, N. S. Electroactive Shape-Memory Polyurethane Composites Incorporating Carbon Nanotubes. *Macromol. Rapid Commun.* **2005**, *26* (5), 412−416.

(18) Yu, K.; Zhang, Z.; Liu, Y.; Leng, J. Carbon nanotube chains in a shape memory polymer/carbon black composites: To significantly reduce the electrical resistivity. *Appl. Phys. Lett.* **2011**, *98* (7), 074102.

(19) Leng, J.; Lv, H.; Liu, Y.; Du, S. Electroactivate Shape-Memory Polymer Filled with Nanocarbon Particles and Short Carbon Fibers. *Appl. Phys. Lett.* **2007**, *91* (14), 144105.

(20) Zhang, D.; Chi, B.; Li, B.; Gao, Z.; Du, Y.; Guo, J.; Wei, J. Fabrication of Highly Conductive Graphene Flexible Circuits by 3d Printing. *Synth. Met.* **2016**, *217*, 79−86.

(21) Leng, J. S.; Lan, X.; Liu, Y. J.; Du, S. Y.; Huang, W. M.; Liu, N.; Phee, S. J.; Yuan, Q. Electrical Conductivity of Thermoresponsive Shape-Memory Polymer with Embedded Micron Sized Ni Powder Chains. *Appl. Phys. Lett.* **2008**, *92* (1), 014104.

(22) Zhang, F. H.; Zhang, Z. C.; Luo, C. J.; Lin, I-T.; Liu, Y.; Leng, J.; Smoukov, S. K. Remote, Fast Actuation of Programmable Multiple Shape Memory Composites by Magnetic Fields. *J. Mater. Chem. C* **2015**, *3* (43), 11290−11293.

(23) Liu, Y.; Boyles, J. K.; Genzer, J.; Dickey, M. D. Self-Folding of Polymer Sheets Using Local Light Absorption. *Soft Matter* **2012**, *8* (6), 1764−1769.

(24) Nambiar, S.; Yeow, J. T. Conductive Polymer-Based Sensors for Biomedical Applications. *Biosens. Bioelectron.* **2011**, *26* (5), 1825−32.

(25) Cho, S. I.; Lee, S. B. Fast Electrochemistry of Conductive Polymer Nanotubes: Synthesis, Mechanism, and Application. *Acc. Chem. Res.* **2008**, *41* (6), 699−707.

(26) Zhang, F.; Zhang, Z.; Liu, Y.; Leng, J. Electrospun Nanofiber Membranes for Electrically Activated Shape Memory Nanocomposites. *Smart Mater. Struct.* **2014**, *23* (6), 065020.

(27) Yu, Z.; Niu, X.; Liu, Z.; Pei, Q. Intrinsically Stretchable Polymer Light-Emitting Devices Using Carbon Nanotube-Polymer Composite Electrodes. *Adv. Mater.* **2011**, *23* (34), 3989−3994.

(28) Yang, C.; Liu, P.; Wang, T. Well-Defined Core-Shell Carbon Black/Polypyrrole Nanocomposites for Electrochemical Energy Storage. *ACS Appl. Mater. Interfaces* **2011**, *3* (4), 1109−14.

(29) Huang, J.; Yang, Z.; Feng, Z.; Xie, X.; Wen, X. A Novel Zno@Ag@Polypyrrole Hybrid Composite Evaluated as Anode Material for Zinc-Based Secondary Cell. *Sci. Rep.* **2016**, *6*, 24471.

(30) Omastová, M.; Trchová, M.; Kovářová, J.; Stejskal, J. Synthesis and Structural Study of Polypyrroles Prepared in the Presence of Surfactants. *Synth. Met.* **2003**, *138* (3), 447−455.

(31) Liu, J.; Wan, M. Composites of Polypyrrole with Conducting and Ferromagnetic Behaviors. *J. Polym. Sci., Part A: Polym. Chem.* **2000**, *38* (15), 2734−2739.

(32) Rana, S.; Kim, S. D.; Cho, J. W. Conducting Core-Sheath Nanofibers for Electroactive Shape-Memory Applications. *Polym. Adv. Technol.* **2013**, *24* (7), 609−614.

DOI: 10.1021/acsami.8b12743
ACS Appl. Mater. Interfaces XXXX, XXX, XXX−XXX